Solution Processed Cu_2ZnSnS_4 Thin Films for Solar Cell Applications

A thesis submitted
in partial fulfillment of the requirements for
the award of degree of

MASTER OF PHYSICS
at
Thapar University, Patiala

Submitted by
PREETI GUPTA
Roll No.301404021

Under the guidance of
Dr. Bhaskar Chandra Mohanty
Associate Professor
School of Physics and Materials Science
Thapar University, Patiala

SCHOOL OF PHYSICS AND MATERIALS SCIENCE
Thapar University
Patiala -147004, India

CERTIFICATE

I hereby declare that the project work is an authentic record of our work carried out at Thapar University, Patiala as required for six months project semester for the award of degree of **M.Sc Physics** from Thapar University, Patiala, under the guidance of Dr. B.C. Mohanty for the period of six months i.e. from January 2016 to June 2016.

Date: June 29, 2016

Preeti Gupta
301404021

It is certified that the above statement made by the student is correct to the best of my knowledge and belief.

(Dr. B. C. Mohanty)
Associate Professor
School of Physics and Material Science
Thapar University, Patiala-147004 (Punjab)

(Dr. Manoj Kumar Sharma)
Professor & Head
School of Physics and Material Science
Thapar University, Patiala -147004 (Punjab)

Dr. S. S. Bhatia
Dean of Academic Affairs
Thapar University, Patiala

DECLARATION

I hereby declare that the work being presented in this thesis report entitled **"Solution Processed Cu_2ZnSnS_4 Thin Films for Solar Cell Applications"** by me in partial fulfillment of the requirements of the award of degree of **Master of Science** in **Physics** from **School of Physics and Materials Science**, Thapar University, Patiala is an authentic record of my work carried out under the supervision of **Dr. B.C. Mohanty, Associate Professor, School of Physics and Materials Science, Thapar University**.

ACKNOWLEDGEMENTS

I would like to express my deep sense of gratitude to Dr. B.C. Mohanty, *Associate Professor School of Physics and Materials Science, Thapar University, Patiala* for his invaluable suggestion, excellent supervision, constant encouragement, thought provoking and unabashed discussion in nurturing the work and during the preparation of manuscript throughout the research work.

My sincere thanks to Dr. Manoj Kumar Sharma, *Professor and Head, School of Physics and Materials Science, Thapar University, Patiala* for providing me with the opportunity to conduct this work and bring it out in the present form.

I offer special thanks and regards to Ms. Indu Gupta and Mr. Jasjit Singh, *Research Scholars, School of Physics and Materials Science, Thapar University,* Patiala for providing immense support in performing, characterizing and evaluating the thesis work.

I would also like to thank my friends (Nidhi and Anisha) for their kind support and encouragement. The greatest thanks go to my family members for their infinite support at each and every part of my life. Above all, I express my indebtedness to the almighty for all his blessing and kindness.

Preeti Gupta

301404021

ABSTRACT

This thesis concerns with the growth and characterization of Cu_2ZnSnS_4 (CZTS) thin films for solar cell application. In the last few years, thin films of CZTS have attracted significant research interest owing to its earth-abundant constituents, high absorption coefficients in the visible region of solar radiation, fairly high tolerance to stoichiometric deviations and presence of native defects which are actually beneficial. The CZTS thin films were prepared using the chemical bath deposition (CBD) technique from non-toxic solutions in contrast to the hydrazine - a very toxic and carcinogenic compound - based solution based techniques, which have yielded the record efficiency.

In this work, the bath solution was prepared from copper chloride as a source of copper ions (Cu^{2+}), zinc chloride as a source of zinc ions (Zn^{2+}), tin chloride as a source of tin ions (Sn^{2+}) and thioacetamide (TAA) as a source of sulfur ions (S^{2+}) and MEA as a complexing agent. The as-deposited films were ex-situ sulfurized at different temperatures to obtain good quality films. The prepared samples were characterized by several techniques such as X-ray diffraction, scanning electron microscopy and UV-visible spectroscopy. The results show that post-deposition sulfurization at 450 °C results in the formation of a single phase polycrystalline CZTS. However, the films were discontinuous with the film surface consisting of sub-micrometer size particles. It shows that although a single dip coating followed by sulfurization at 450 °C yields polycrystalline CZTS, further processing in the form of multiple coating is required for developing microstructure suitable for photovoltaic applications.

CONTENTS Page no.

Chapter 1: INTRODUCTION 1

1.1 Issues of the energy economy 1

1.2 Why solar energy? 1

1.3 Thin film photovoltaics 2

1.4 Possible materials 2

1.5 Cu_2ZnSnS_4 compounds as alternative to CIGS 4

1.6 CZTS thin films 4

1.6.1 Structural Properties 5

1.6.2 Electrical properties 6

1.6.3 Optical properties 6

1.7 Literature review on CZTS thin films 7

1.8 Chemical bath deposition (CBD) method for fabrication of CZTS thin films 9

1.9 Motivation and Objectives 10

Chapter 2: EXPERIMENTAL TECHNIQUES 12

2.1 Growth of CZTS thin film 12

2.2 Characterization techniques 15

2.2.1 Structural characterization using X-Ray diffraction (XRD) 15

2.2.2 Surface microstructure studies by FESEM 16

2.2.3 Optical transmittance and band gap measurements 16

Chapter 3: CHARACTERIZATION OF CZTS THIN FILMS 19

3.1 Structural Studies using XRD 19

3.2 Evaluation of surface and cross-sectional microstructure 20

3.3 Optical studies 24

Chapter 4: SUMMARY AND FUTURE SCOPE 26

REFERENCES 27

LIST OF FIGURES

Figure	Title	Page
1.1	On gradually substitution of elements to get the various possible compound semiconductors.	3
1.2	Schematic representations of the kesterite (a) and stannite (b) structures [112]	5
1.3	Film deposition set-up using CBD method	10
2.1	Photograph of prepared solutions of 10 ml each of copper chloride, zinc chloride, tin chloride and 20 ml of TAA	12
2.2	Photograph taken after adding MEA in first three solutions	13
2.3	Photographs of solutions showing colour changes during the CBD process **(a)** only copper solution, **(b)** after adding zinc solution, **(c)** after adding tin solution, **(d)** final solution after adding TAA	14
2.4	Showing colour change of solution from 0 to 30 min	15
2.5	Illustration of the constructive interference of the X-rays scattered from lattice planes.	16
2.6	Single Beam UV-visible spectrophotometer	18
2.7	Double Beam UV- visible Spectrophotometer	18
3.1	XRD patterns of the as-deposited and sulfurized samples. The Miller indices of the corresponding peaks have been indexed.	19
3.2	Typical surface and cross-sectional FESEM images of the as-deposited films.	21
3.3	Typical surface and cross-sectional FESEM images of the film sulfurized at 400 ºC.	22
3.4	Typical surface and cross-sectional FESEM images of the film sulfurized at 450 ºC.	23
3.5	Optical transmittance curves of the as-deposited and sulfurized CZTS films.	24

CHAPTER 1
INTRODUCTION

1.1 Issues of the energy economy

With industrialization and changed living style of an ever-increasing world population, there are growing concerns on how to meet the energy demand and the security there of. At current time, there is a big gap between the amount of energy produced and that required for sustainable civilization. So far, the main source of the energy has been coal and oil from the conventional fossil energy [1]. However, for these conventional resources of energy being exhaustible and the political parties are using the fossil fuel resources for there own purposes, there are growing apprehensions that it may adversely affect global financial and social development [2]. This energy crisis is much more severe for developing countries including India whose national budget for development programs will be used for purchasing petroleum products. Furthermore, greenhouse gas emission from fossil fuel is causing global warming, which is also a matter of great concern [3].

To resolve theses issues of conventional resources of energy, mostly developing countries are trying to find other non-conventional source of energy which is also renewable source such as sunlight, wind energy, geothermal, rain, and small hydroelectricity.

1.2 Why solar energy?

Modern movements propose that in future solar power will take a very important part in production of energy. The sun delivers electromagnetic radiation of order ~ 120,000 TW on the Earth's surface, which is more than human needs. Even by using 10 % efficient solar conversion systems, we will get 20TW of power by just covering 0.16 % of the Earth's land, which is almost two times the consumption rate of fossil energy of whole world at present [4-6]. This comparison shows the incredible magnitude of the solar resource, which, if harnessed, can end the energy woes.

Devices that convert solar energy to electrical energy provide many benefits like pollution-free, reliable, self-contained, noise-free, durable, maintenance-free, and works for long term continuously and limitless operation at bearable costs. Even with these blessings, solar cells and solar panels contribute to world's electricity only about 0.04 %, the prime reason for this

being its high cost [7]. However, there are increasing efforts to understand and develop new materials for photovoltaic (PV), to design low cost new fabrication techniques and to enhance existing efficiencies by manipulating material properties, which can make the PV technology more affordable.

1.3 Thin film solar cells

The solar cell industries have been developing over current time with the vending of products based on the Si wafers. As mentioned above, the key factor that affects the acceptability of PV technology in domestic and industrial sectors is its cost. In the case of Si based devices, the cost of the wafer is half of the overall panel cost. There is a way to solve high cost element problem, if we deposit thin films of semiconducting material on some substrate instead of using wafers [8], which work efficiently.

The other motivation, apart from less material consumption, for using thin film solar cells is, it has the possibility for high speed manufacturing [9]. Typical thin film absorber materials have the absorption coefficient 100 times higher than crystalline Si and equivalent amount of energy can be absorbed by thin film materials with 100 times thinner absorber layer than crystalline Si. For example, to make a 1 m^2 solar cell, only 1cm^3 of thin film material against 100 cm^3 of crystalline Si is needed. In addition, compared to crystalline Si solar cells, purity and other parameter requirements of thin film solar cells are not rigid [10]. Hence, thin film absorber layer solar cells can be manufactured at moderate prices. Another interesting asset of thin film solar cells, flexible materials can be used as substrate like on metal foils, which open whole new branch of applications. As far as thin film material properties are concerned, by varying composition, the band gap of thin film materials can be adjusted to our requirement, which enables one to utilize the larger part of the solar spectrum and achieve of higher efficiency.

1.4 Possible materials

For thin absorber layer solar cells, there are various significant situations which should be satisfied by the compound: (i) A large absorption coefficient, which ensures that most of the available photons are absorbed in a short distance i.e. a few micrometers, (ii) An appropriate band-gap vary from 1 eV - 1.7 eV (according to theoretical calculation to get enough energy). As can be seen by the **Figure 1.1**, these conditions can be fulfilled by quite a lot of materials. Si has

been the most popular choice among the semiconductors. In thin film solar cell technology, the most suitable, however, is amorphous Si (a-Si). The properties of crystalline Si are different from amorphous Si which is a disordered material. There is an increment in the value of band-gap occur, from 1.1 eV for crystalline Si to 1.7 eV for a - Si. Absorption coefficient value is relatively higher in case of a-Si than for crystalline Si.

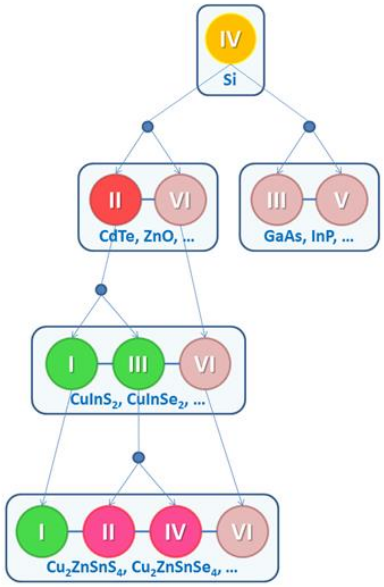

Figure 1.1 On gradually substitution of elements to get the various possible compound semiconductors.

When it gets mandatory to find another material, an approach that is often followed is the method of isoelectronic/cross substitution [11]. Using the cross substitution method, group IV (silicon) atoms are replaced by similar no. of anions and cations of group V and group III or group VI and II respectively to make organogallium compound or cadmium telluride which are binary compounds. To form additional compound semiconductors, group-II element can be substituted by half of the group-I elements and half of the group-III element. For e.g, I-III-VI compound semiconductor material will be ($CuInSe_2$) or by replacing some of the 'In' by 'Ga', band gap can be modified to form a new compound naming $CuInGaSe_2$ (CIGS). Furthermore substitutions can also be carried out, for example on partially replacing the group-III element by group-II elements and other left part with a group-IV element. Moreover, it should be taken care of that not all substitutional compounds may work. But only those will work which form

appropriate junction with new materials and show photovoltaic effect on exposure to light are good for thin film photovoltaic applications.

1.5 Cu_2ZnSnS_4 compounds as alternative to CIGS

Among various thin film photovoltaic devices, $Cu(In,Ga)(S,Se)_2$ (CIGSSe) and CdTe solar cells have shown record efficiencies of 20.8 % and 20.4 % [12-13], respectively, but there industrial panels have reached efficiencies of values as 17.8 % and 17.0 % [14-15]. Despite the promise of CIGS and CdTe thin film technologies, the low abundance of elements like indium and tellurium limit their suitability in large scale production and in making them cost-competitive. In the last two decades, efforts are going on to find a new branch of quaternary compounds so we can compensate CIGS compound for absorber layer in solar cells. These new compounds can be studied as a descent of CIGS compound of chalcopyrite type. By using the above process of cross substitution, replacing one element (indium or gallium in the latest case) with two elements of separate groups of the periodic table, while taking care of the ratio of the no. of atoms present and valence negatively charged electrons, a number of quaternary compounds with formula Cu_2-II-IV-VI_4, here VI is a chalcogen element (Sulfur) while II and IV are divalent having a valency of two (zinc, cadmium, iron) and tetravalent having valency of four (germanium, silicon, tin) elements, respectively, can be considered. Among all possible Cu_2-II-IV-VI_4 compounds, kesterite Cu_2ZnSnS_4 (CZTS) is the most studied one and in recent years, its improvement in photovoltaic performance makes it more attractive.

In addition to the earth abundant, non-toxic (safe), and inexpensive constituents, CZTS exhibits a high absorption coefficient of ~10^4 cm^{-1} and a tunable band gap (vary from 1 to 1.5 eV) that can nicely match the solar spectrum [16-17]. Thus, the CZTS material appears to be both economically and ecologically viable without serious constraints from raw materials. In the last few years intensified research on CZTS material has progressed its energy conversion efficiency from about 6.8% in 2008 [18] to beyond 12% just in a few years [19].

1.6 CZTS thin films

Lately considerable amount of efforts has already been done on the thin films of CZTS and has been found to be potential absorber layer for thin film solar cells [20-21]. CZTS shows desired physical properties such as a band-gap of ~ 1.5 eV, a high value of optical absorption

coefficient >10^{-4} cm^{-1}, high thermal resistivity, etc. Since, copper zinc tin sulfide is descent of the CIGS compound by using the method of cross substitution, by replacing two 'indium' atoms by one of the 'zinc' and one 'tin' atom, CZTS compound has some comparable effects as that of CIGS. In the followings, a few of the properties have been highlighted.

1.6.1 Structural Properties

CZTS compounds is reported to exist in two structures, namely kesterite and stannite type [22]. Both of these structures are identical except the positioning of copper and zinc atoms is different (**Figure 1.2**). Both consist of a cubic closed packed array of sulphur anions having tetragonal structure, with cations carrying one half of the tetrahedral voids. This stacking is similar to zinc blende. However, CZTS is usually found in kesterite phase due to the reason that it is thermodynamically more stable than stannite phase [23-24]. The values of lattice constant for CZTS are a = 0.54 nm and c = 1.09 nm [25]. From this one can find the density (using the atomic masses of 'copper', 'zinc', 'tin' and 'sulfur') of CZTS as ~ 4.6g/cm^3 [26].

Washio et al. [27] examined CZTS thin films for their correlation between composition and kesterite structure. They considered three different ratios of compositions of Cu/(Zn+Sn) as 1.2, 1.0, and 0.8. It was seen that when the ratio is 0.8, 'copper' alternates for 'zinc' at the 2d site and/or 'zinc' alternates for 'copper' at the 2c site. They believed that CZTS thin film photovoltaic activity shows high performance due to its kesterite crystal structure.

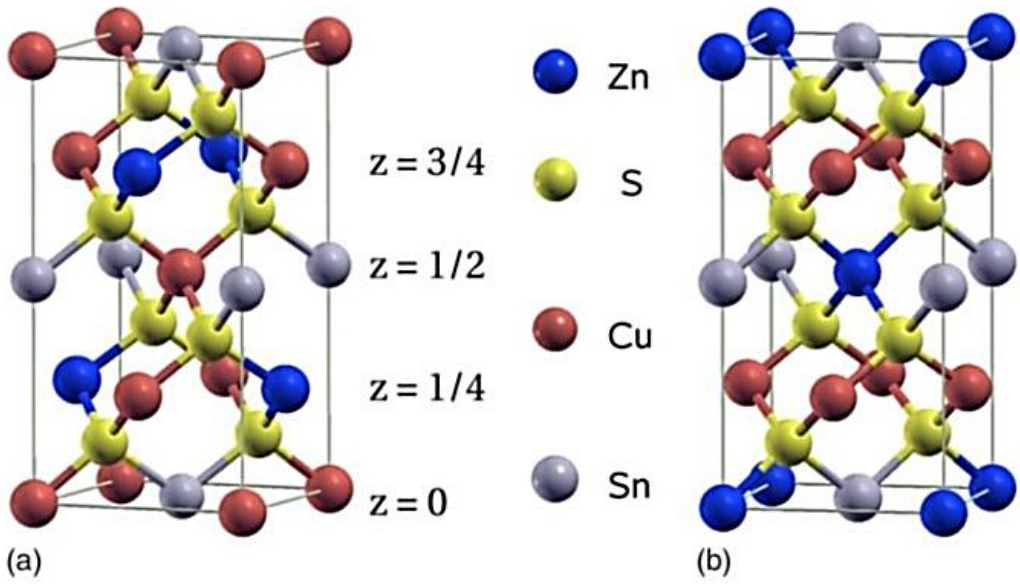

Figure 1.2 Schematic representations of the kesterite (a) and stannite (b) structures [112]

1.6.2 Electrical properties

When CZTS material is doped, it happens by means of internal defects. According to first principle theoretical computations of the transition energy levels and the formation energy with a series of defect complexes and intrinsic point defects in copper zinc tin sulfide shows that *p*-type conductivity is due to the 'copper' atoms sitting on the places of 'zinc' atoms which carry lower value of formation energy and comparably deeper acceptor level as compared to 'copper' vacancy [28]. Higher formation energy of all donor defects is uniform with the experimental data of p-type conductivity. In CZTS, N-type doping is tough due to low formation energy of acceptor defects.

Most reported values of copper zinc tin sulfide thin films resistivity differ from ~10^{-3} Ω.cm to 10^{1} Ω.cm [21, 29-33] but highest value of resistivity 10^{4} Ω.cm were also claimed [34]. Concentration of holes was noted to vary from 10^{16} cm^{-3} to 10^{21} cm^{-3} [35-38]. From Hall Effect results, it was seen that mobility of holes changed from 0.1 to 30 $cm^{2}V^{-1}s^{-1}$ in CZTS, most reported values were in the range of 1 to 10 $cm^{2}V^{-1}s^{-1}$[37-41]. Lower mobility value shows that the advanced thickness of copper zinc tin sulfide thin film solar cells absorber layer cannot be larger than copper indium gallium selenide thin film absorber layer photovoltaic.

1.6.3 Optical properties

Apparently calculated value of band-gap of kesterite type copper zinc tin sulfide (CZTS) is 1.5 eV by Chen et al. [42]. At experimental lattice constants, they performed hybrid functional calculations (HSE06), where one fourth percent of the generalized gradient approximation exchange potential is placed. By using various deposition techniques, the band-gap reported varied in the range 1.4 eV to 1.55 eV [38, 43-46]. Low value as 1.2 eV is also noted on divergence in stoichiometry [47].

The value of absorption coefficient of copper zinc tin sulfide thin films is >10^{4} cm^{-1} [48, 49]. When CZTS absorber layer was fabricated with 75 mW of RF power using RF magnetron sputtering method, a refractive index of 2.07 was observed with annealing at 400 ^{0}C is reported by Seol et al. [43]. Many researchers are trying to find the recombination mechanism happen in CZTS absorber layer by studying the low temperature photoluminescence spectra. A broad peak having center at nearly equal to 1.2 eV is seen in most of the reports. A model was proposed by Leitao et al. [50-51] in which radiative recombination was broadened of an electron recombining

with a hole which is present in an acceptor level by means of potential fluctuations occurring in the valence-band edge. Photoluminescence was assigned to activation energy of 39 meV and 59 meV for CZTS and Copper-poor, Zinc-rich respectively for donor-acceptor pair recombination.

1.7 Literature review on CZTS thin films

The photovoltaic effect of CZTS material was reported in 1988 by Ito and Nakazawa [52]. They made a heterodiode using Cu_2ZnSnS_4 and cadmium tin oxide thin films on stainless steel substrates. The CZTS thin film used in study was deposited by atom beam sputtering from pressed targets of CZTS. The band gap of CZTS was 1.45 eV, an optimum value for the photo-absorber layer of a single junction solar cell. In 1997, Katagiri et al. showed that the films had a stannite structure. They estimated the optical absorption coefficient to be order of $10^4 cm^{-1}$ and optical band gap of 1.45 eV having p-type conductivity [53]. Moreover in 1997, Friedlmeier et al. made absorber layer for solar cells with conversion efficiency 2.3%, with the CZTS absorber layer synthesized by the sulfidation of co-deposited Copper-Zinc-Tin films [54]. In 1999, Katagiri's group broke this record with a CZTS film with conversion efficiency 2.63% by trying different way they sulfidized the copper/tin/zinc-sulfide stacks [55]. In 2003, they further improved the efficiency of solar cell to 5.45% by boosting the sulfurization process. They reported that the improvement in the efficiency was mainly due to higher vacuum during sulfidization that reduced the contamination from the residual gas [56]. In 2010, Todorov et al. reported conversion efficiency of CZTS to be 9.6% using a composite liquid deposition approach combining the concepts of solution based and particle based coating [57]. In 2013, a world-record for CZTSSe solar cell with a conversion efficiency of 12.6% from hydrazine based solution process was reported [19].

As referred above, variety of methods have been used to fabricate the CZTS thin films for photovoltaic applications. Compared to the vacuum based methods, which are relatively expensive, more recently non-vacuum based methods have become popular for commercial production. In addition to its cost competitiveness, the solution based methods offer other advantages of easy control of process parameters, low temperature and large area deposition, and high throughput. In this work, a solution based approach was used to fabricate CZTS thin films, similar to the one already in use by many research groups.

Till date, three routes have achieved popularity among the various solution-based processes to synthesize CZTS thin films. In the 1st approach, there put inks in layers form having CZTS nanocrystals which is annealed at particular temperature in Selenium atmosphere to make CZTSSe [58]. With amendment of the elemental ratios, it can give devices with 7.2% efficiency [59]. While it is easier to prepare the film due to dispersibility of the nanocrystals in organic solvents, the resulting encapsulating organic ligands often leave C-atom behind that limit the device activity [60]. In the 2nd approach, binary chalcogenides are first synthesized and then scattered in hydrazine. Using this hydrazine based slurries having both soluble and particular precursor, the CZTSSe absorber layer has been deposited directly. With this approach, the efficiency of 12.6 % for any CZTSSe preparation process [19]. The third approach is based on deposition from a homogeneous solution of fully dissolved CZTS precursor. Compared to the nanocrystal inks and slurry based processes, the homogeneous solution method is advantageous owing to mixing at a scale of molecular levels and hence, offer very accurate stoichiometric control and save us from the need for the thorough diffusion of precursors during the fabrication of the CZTS phase. In the followings a few of the reports concerning with the fabrication of the CZTSSe thin films from the clear non-hydrazine solutions have been highlighted.

Fischereder et al. prepared the CZTS thin film using toxic pyridine-based solution [61]. Ki et al. and Choudhury et al. used dimethyl sulfoxide (DMSO) and methanol as solvent for Cu, Zn, Sn salts and thiourea for synthesizing CZTS thin films [62]. There was a problem related to thiourea (at high annealing temperature of 380^0C), it tend to form organic by-products [63]. Sun et al. synthesized CZTS thin films using a simple process of multiple dip coating with usage of non-toxic alcohol based homogenous solution, which was expected to reduce the carbon content [64]. They reported the efficiency to be 5.36 %. Sutter-Fella et al. fabricated CZTS thin films using chemical solution processing [65]. They observed poor crystallinity shown by the chalcogenide absorber layer by this method. They used sodium containing reactive agent to overcome this drawback and showed a massive enhancement in grain growth. Due to this, its semiconductor properties get modified and can be maximized by adjusting the sodium precursor quantity. They reported an efficiency to be 6.04 %. To study the effect of alkali atoms, a similar approach was carried out by Tong et al. by using potassium instead of sodium [66]. They prepared CZTS thin films using metal acetate and thiourea in methanol and ethanoldiamine as solvent by spin coating technique. They showed an enhancement of (112) orientation, an

increase in grain size, reduction in the secondary phase, decrease in R_S and improved value of J_{SC}. They noticed an improvement in efficiency from 2.94 % to 3.34 % on adding 1 % potassium in precursor compared to undoped films. Park et al. tried to prepare uniform CZTS thin films by adding/removing organic chemicals [67]. They used the spin coating technique to prepare CZTS layer from metal chlorides and multi-functional thiourea in ethanol as solvent. Thiourea was used both as a source of sulphur and a stabilizer because it forms complexes with metal chlorides. Recently, Nguyen et al. synthesized CZTS thin films using precursor solution prepared from metal chloride and thiourea in water and ethanol by spin coating technique [68]. Using a two-zone tube furnace, they then sulfurized the prepared films and showed that on the surface of CZTS layer, metal sulfates of various clusters were partially embedded. Yang et al. deposited CZTS thin films using water based precursor solution [69]. They used powdered Cu, Zn, Sn, and S dissolved in thioglycolic acid and methylamine based aqueous solution and deposited CZTS nanocrystal thin film from homogeneous precursor solutions. They reported photovoltaic conversion efficiency of 6.96 % and open-circuit voltage of 378mV. Prabeesh et al. studied the effect of annealing temperature on CZTS absorber layer [70]. They made CZTS by one step solution based method using harmless chemicals by spin coating and also find the effect of annealing temperature in nitrogen atmosphere. They reported good crystallinity, dense structure, band gap value to be 1.49 eV and absorption coefficient of 10^4 cm^{-1} for samples annealed at 500 ^{0}C for 30 min.

1.8 Chemical bath deposition (CBD) method for fabrication of CZTS thin films

As presented above, in literature one can find a number of solution based techniques used for deposition of the CZTS thin films with varied success. The CBD process which has been traditionally known for low cost, high throughput and large area deposition of uniform thin films of various materials of technological importance has been used in this work.

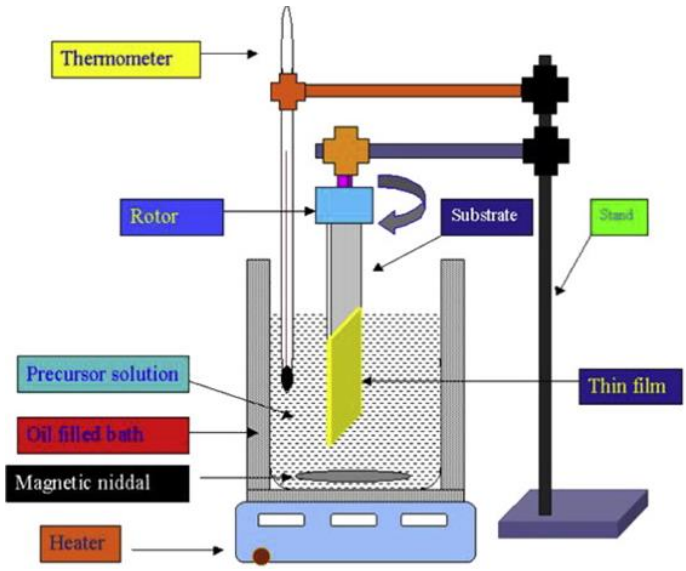

Figure 1.3 Film deposition set-up using CBD method

By taking care of composition and molarity of all the components, solutions are prepared. Mixing all these solutions step by step, a final solution is prepared. In **Figure 1.4**, the setup of chemical bath deposition is shown. Thin films are deposited on glass substrate immersed in the solution. Typically, properties of the deposited films are strongly dependent on the time duration of deposition, bath temperature, initial precursor solution concentration, etc. The as-deposited film has to be dried, resulting in a uniform and well-adherent films. The process of film preparation has been presented in detail in Chapter 2.

1.9 Motivation and Objectives

The literature review presented above shows solution based techniques have yielded CZTS thin films of better performance. However, the high efficient CZTS based solar cells involve hydrazine based solutions, which is toxic and carcinogenic. Hence, there have been heightened efforts in fabrication of CZTS thin films by solution processes without hydrazine. As discussed above, chemical bath deposition process is simple and inexpensive, and hence was chosen as the method of fabrication of the films. The objectives of this work are

- Growth of CZTS thin films using a non-toxic homogeneous precursor solution based method such as CBD and study of effect of post-deposition sulfurization temperature on film properties.

- Investigation of the structural, surface properties and optical properties of the resulting CZTS thin films

The thesis is organized in the following manner: Chapter 1 gives a brief introduction to the material of interest, i.e. CZTS, and motivation and objectives of the work. Chapter 2 presents the experimental techniques used for the growth and characterization of the films. In Chapter 3, the results and discussion have been presented. A brief conclusion is presented in Chapter 4 followed by references.

CHAPTER-2
EXPERIMENTAL TECHNIQUE

In this chapter, experimental techniques pertaining to the growth of the CZTS thin films and their characterization are presented. In Section 2.1, a description is given about the method of preparation of the films. In Section 2.2, the detail of the various methods used to characterize the thin films.

2.1 Growth of CZTS thin film

In this work, CZTS thin films were prepared by the CBD method. A generic scheme of film deposition by CBD has been presented in section 1.8. In this section, the specific experimental conditions and procedure for the growth of thin films are described.

Copper chloride as a source of copper ions (Cu^{2+}), zinc chloride as a source of zinc ions (Zn^{2+}), tin chloride as a source of tin ions (Sn^{2+}) and thioacetamide (TAA) as a source of sulfur ions (S^{2+}) and MEA as a complexing agent were used. Firstly, stock solutions of 0.25 M $CuCl_2$, 0.125 M $ZnCl_2$, 0.125 M $SnCl_2$, 1 M TAA and 0.04 mM of MEA were prepared in ethanol. **Figure 2.1** shows photographs of the prepared solutions. Then, 10 ml of MEA solution was added to each of 10 ml $CuCl_2$ solution, 10 ml of $ZnCl_2$ solution and 10 ml of $SnCl_2$ solution individually as shown in **Figure 2.2**. Hence, 20 ml of each cation solution is prepared.

Figure 2.1: Photograph of prepared solutions of 10 ml each of copper chloride, zinc chloride, tin chloride and 20 ml of TAA

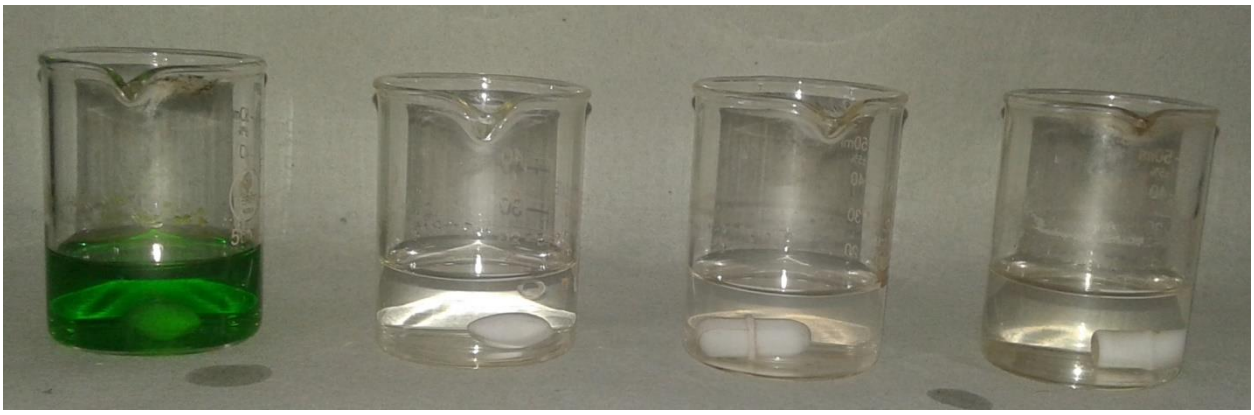

Figure 2.2: photograph taken after adding MEA in first three solutions

The sequence of adding solutions were: copper chloride, zinc chloride and tin chloride as shown in **Figure 2.3**. Stirring of the solution was maintained at 600 RPM. For measuring the temperature, a thermometer (with an accuracy of $\pm$ 1^0C) was kept inside the solution and the bath temperature was maintained at 60^0C. The glass slide was first washed with soap solution, then ultrasonicated cleaning in distilled water and cleansing with acetone for 5 min each. This cleaned glass slide was kept vertically stand in the solution. Then, 20 ml of the prepared TAA solution was added after bath temperature was stabilized at 60^0C. It was noted that the colour of the solution was slowly changed to brown. **Figure 2.4** shows this change in the solution. After 60 min, the substrate with the coating was removed from the solution and was cleaned ultrasonically (1 min) to remove loosely adhered particles followed by the air-drying.

Post-deposition sulfurization of the samples was carried out in a horizontal quartz tube furnace. The temperature of the furnace was controlled by a PID feedback loop to an accuracy of ± 2 °C. The samples were sulfurized either at 400 or 450 °C for a period of 60 min. Prior to heating, the furnace tube was flushed with argon and the sulfurization was carried out in argon atmosphere. After the desired duration of the heat treatment, the furnace was switched off and the sample was allowed to cool naturally under flowing argon gas.

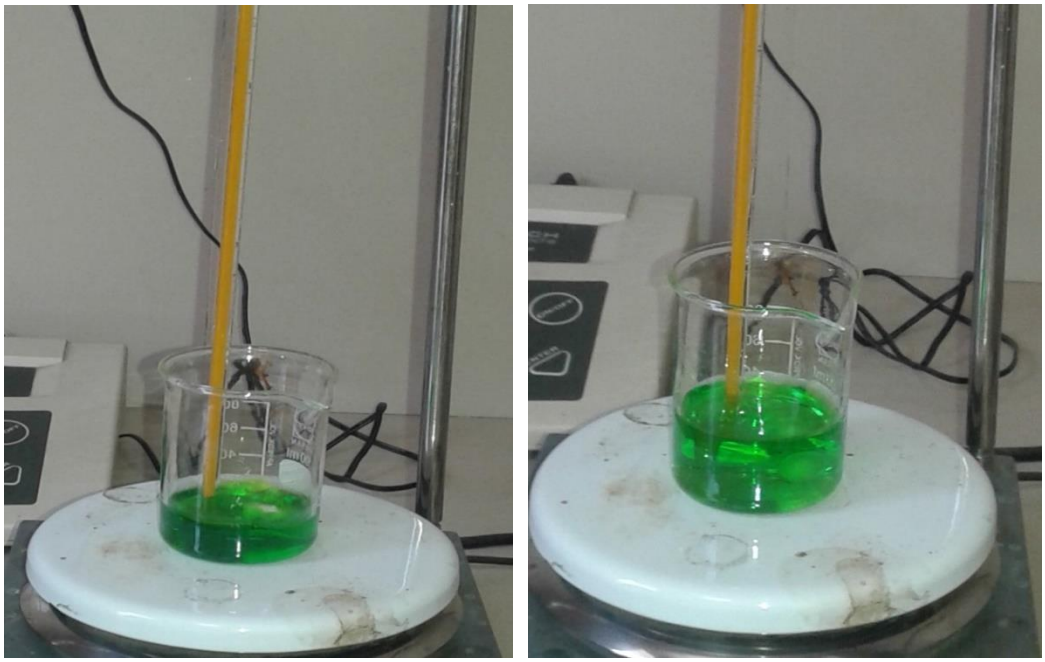

(a) (b)

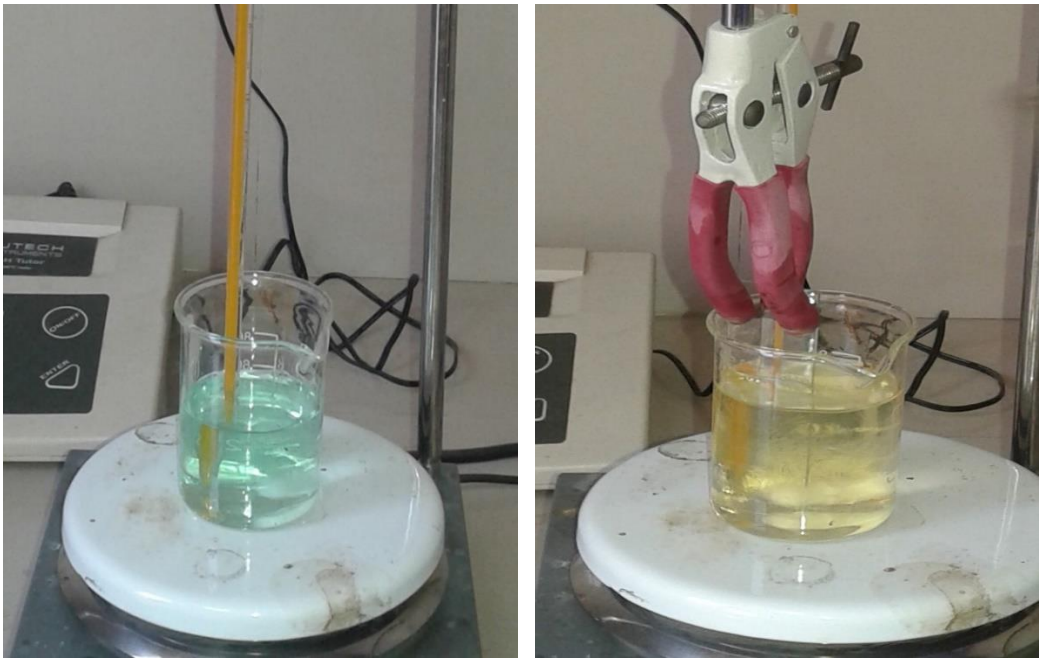

(c) (d)

Figure 2.3: Photographs of solutions showing colour changes during the CBD process **(a)** only copper solution, **(b)** after adding zinc solution, **(c)** after adding tin solution, **(d)** final solution after adding TAA

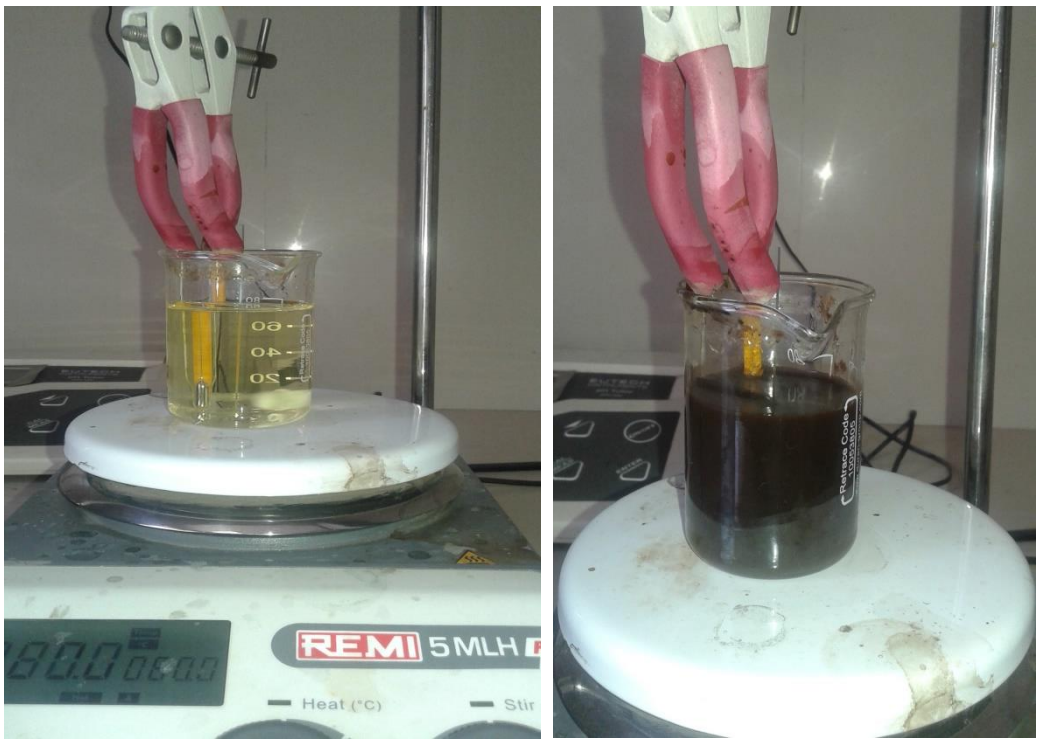

Figure 2.4: Showing colour change of solution from 0 to 30 min

2.2 Characterization techniques

2.2.1 Structural characterization using X-Ray diffraction (XRD)

X-ray diffraction analysis is a unique method for the determination of crystallinity of a compound. Diffractogram result from XRD measurement shows the intensity as a function of the diffraction angles. The basis of the XRD is the constructive interference of monochromatic X-rays scattered by atoms in different planes of a crystalline sample. Experimentally, cathode ray tube generates X-rays that are filtered to generate monochromatic radiation, and then, collimated to focus and moved towards the sample. When the conditions of Bragg's Law ($n\lambda=2d\sin\theta$) are satisfied, the scattered waves interfere constructively to give a peak at that specific angle. This law relates the diffraction angle to the wavelength of electromagnetic radiation and the lattice spacing in a crystalline sample [74]. From the sets of angles where Bragg reflection peaks were observed, one can determine the structure of the solid. As expected, for a material of amorphous nature, no peaks would be observed. **Figure 2.5** illustrates the basic principle of the XRD.

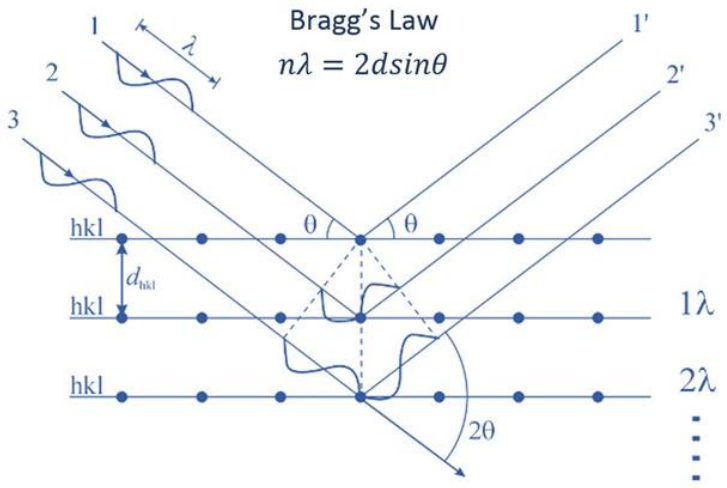

Figure 2.5: Illustration of the constructive interference of the X-rays scattered from lattice planes.

2.2.2 Surface microstructure studies by FESEM

FESEM stands for Field Emission Scanning Electron Microscope. This microscope works with negatively charged electrons instead of light. Field emission source liberates these electrons. Acc. to a zig-zag pattern, the object is scanned by the electrons. A FESEM is useful to picture very tiny topographic features on the surface or fractioned or whole of the objects. Many researchers from all fields like chemistry, biology and physics use this method to visualize structures that can be as small as 1 nm.

In FESEM, electrons which are released from a field emission source are accelerated by the high electrical field gradient. These primary electrons are concentrated in the high vacuum column and diverted by electronic lenses so that to produce a restricted scan beam which strikes the object. Hence object actually emits these secondary electrons. The knowledge of angle and velocity of these electrons are useful to know about structure of the object. A detector is used to catch the secondary electrons and produce a signal. Then the signal is boosted and transformed to a video scan-image that is shown on a monitor or as a digital image which can be saved and further processed [75].

2.2.3 Optical transmittance and band gap measurement

To use thin films for photovoltaic applications, the knowledge about their properties like optical transmittance, absorbance and bandgap is very useful. UV-visible-NIR spectroscopy is

used for this purpose. The principle of UV-visible-NIR spectroscopy is, when a radiation of particular wavelength passes through the material, its intensity will decrease exponentially. According to Beer-Lambert law:

$$I = I_0 e^{-\alpha d} \qquad \ldots\ldots (2.2)$$

Where I_0 is the intensity of the incident light, α is the absorption coefficient and *d* is the thickness of the sample. On rearranging above Eq. (2.2) gives

$$\alpha = -\frac{1}{d} \ln \frac{I}{I_0} \qquad \ldots\ldots\ldots (2.3)$$

the ratio I/ I_0 gives the value of transmittance (T) of the sample. Hence, we can inter-relate the absorption coefficient (α) and the transmittance (T) of the film through the equation

$$\alpha = -\frac{1}{d} \ln T \qquad \ldots\ldots\ldots (2.4)$$

By using the direct allowed transition relation, we can estimate the value of band gap by plotting $(\alpha h\upsilon)^2$ as function of hυ,

$$A = \frac{A_1}{h\upsilon\,(h\upsilon - Eg)^{1/2}} \qquad \ldots\ldots\ldots (2.5)$$

Where A_1 is a constant and E_g is the energy gap. For determining the value of band gaps of semiconducting thin films, plot the graph between $(\alpha h\upsilon)^2$ and hυ, on extrapolating the intercept on the abscissa, value of E_g can be determined [76-78].

A spectrophotometer consists of four main components such as a light source, a sample holder, a monochromator and a detector. Tungsten filament is commonly used as source of light. The detector is simply a photomultiplier tube, a photodiode, a photodiode array or a charge coupled device (CCD). Single photodiode detectors and photomultiplier can detect only a single wavelength of light that reaches it. Scanning monochromators are used to filter the light, so that only one wavelength reaches the detector at one time. With CCDs and photodiode arrays, fixed monochromators are commonly used. In both of the devices, many detectors are placed into one or two dimensional arrays, to make them able to collect light of different wavelengths at different pixels or groups of pixels simultaneously.

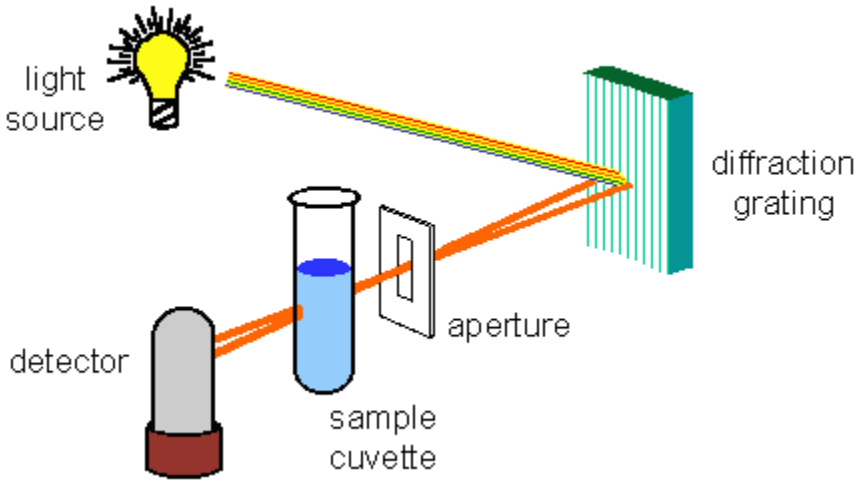

Figure 2.6: Single Beam UV-visible spectrophotometer

Double-beam UV-visible spectrophotometer

In the case of double-beam spectrophotometer, before reaching the sample, the light split's into two beams. One of them is used as reference beam and the other is made to pass through the sample. The intensity of reference beam is taken as 100% transmission (0% absorbance), and that of measurement is displayed as the ratio of two beam intensities.

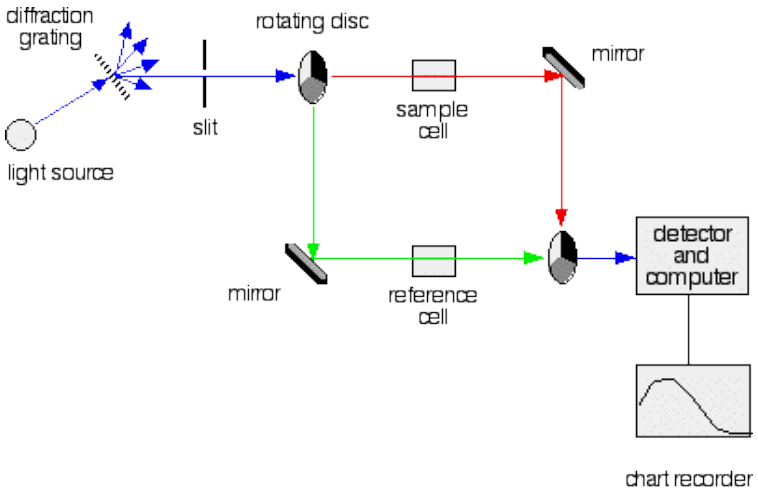

Figure 2.7: Double Beam UV- visible Spectrophotometer

CHAPTER 3
CHARACTERIZATION OF CZTS THIN FILM

This chapter deals with the detailed characterization of the CZTS thin film grown by the CBD method as outlined in the previous chapter.

3.1 Structural Studies using XRD

Figure 3.1 shows typical XRD patterns obtained for the as-deposited and the sulfurized samples. As seen from the figure, XRD pattern of the as-deposited sample is featureless indicating the amorphous nature of the sample However, post-deposition sulfurization induced crystallization, as evident from the appearance of the Bragg peaks in the XRD patterns. As the sulfurization temperature was increased, the peak intensity increased, which suggests improved degree of polycrystallinity with increasing temperature.

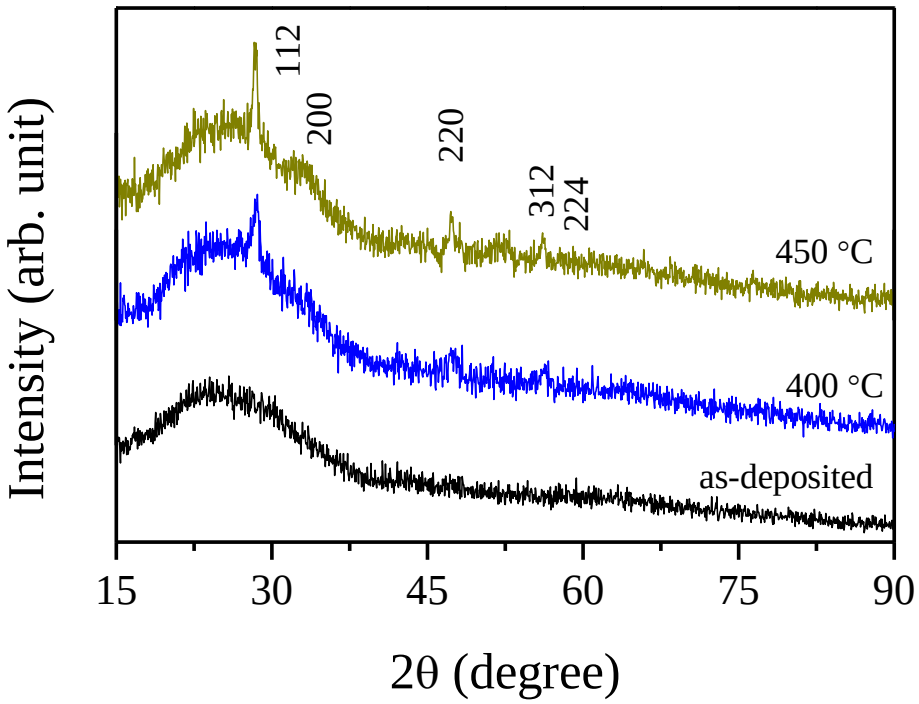

Figure 3.1: XRD patterns of the as-deposited and sulfurized samples. The Miller indices of the corresponding peaks have been indexed.

Analysis of the XRD pattern of the sulfurized samples indicates the formation of single phase kesterite Cu_2ZnSnS_4 of tetragonal structure, as confirmed from the JCPDS (Joint Committee on Powder Diffraction Standards) database with card number 26-0575 [JCPDS Card: 26- 0575]. The peaks located at 2θ values of 28.5^0, 47.3^0 and 56.1^0 respectively corresponding to the reflection from the (112), (220) and (312) planes of CZTS are characteristics of the 'kesterite' structure. The Miller indices, the values of the inter-planar spacing (*d*) of the reported (JCPDS) and calculated (this work) ones, and the reported relative intensities (I/I_0) of the diffraction lines are given in **Table 3.1**. It was found that the JCPDS values and the calculated inter-planar spacing values of this work are in good agreement with each other. Given the inter-planar spacing for a tetragonal system $d = [((h^2+k^2)/a^2) + (l^2/c^2)]^{-1/2}$, the lattice constants of the crystals have been determined. The lattice constants 'a', 'b' and 'c' of the CZTS crystals are a = 5.427 Å, b = 5.427 Å. and c = 10.848 Å.

Table 3.1 X-ray thin film diffraction data for CZTS crystal

(hkl)	**d_{hkl}(Å) (this work)**	**d_{hkl}(Å) (JCPDS data)**	**I/I_0 (%) (JCPDS data)**
112	3.431	3.126	100
220	1.919	1.919	90
312	1.636	1.636	25
224	1.566	1.565	10
200	2.713	2.713	9

3.2 Evaluation of surface and cross-sectional microstructure

The surface and cross-sectional microstructure of the as-deposited and sulfurized samples were examined by FESEM as mentioned in chapter 2. The SEM micrographs corresponding to the as-deposited sample is shown in **Figure 3.2**. At low magnification, the film appears to be continuous and fully covers the substrate. Some occasional particulates (lighter contrast in the micrographs) are also visible. However, as the magnification was increased, a uniform mesh-like surface structure was observed. The particulate aggregates on the surface are also of same microstructure. The cross-sectional image shows the thickness to be about 210 nm.

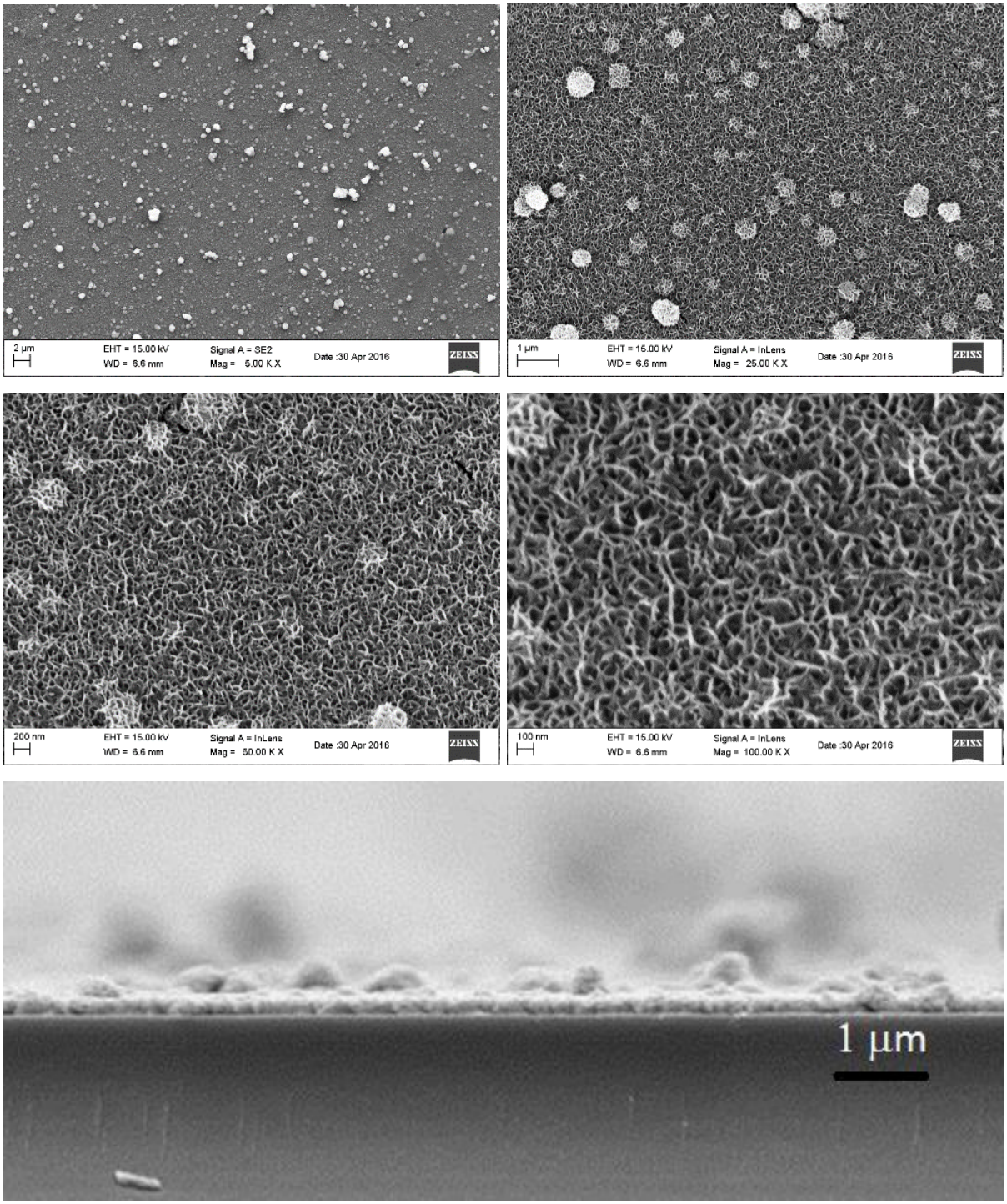

Figure 3.2: Typical surface and cross-sectional FESEM images of the as-deposited films.

However, as the samples were sulfurized, the microstructure of the samples were drastically changed. The surface and cross-sectional images of the films sulfurized at 400 and 450 ºC are shown in **Figure 3.3 and 3.4** respectively.

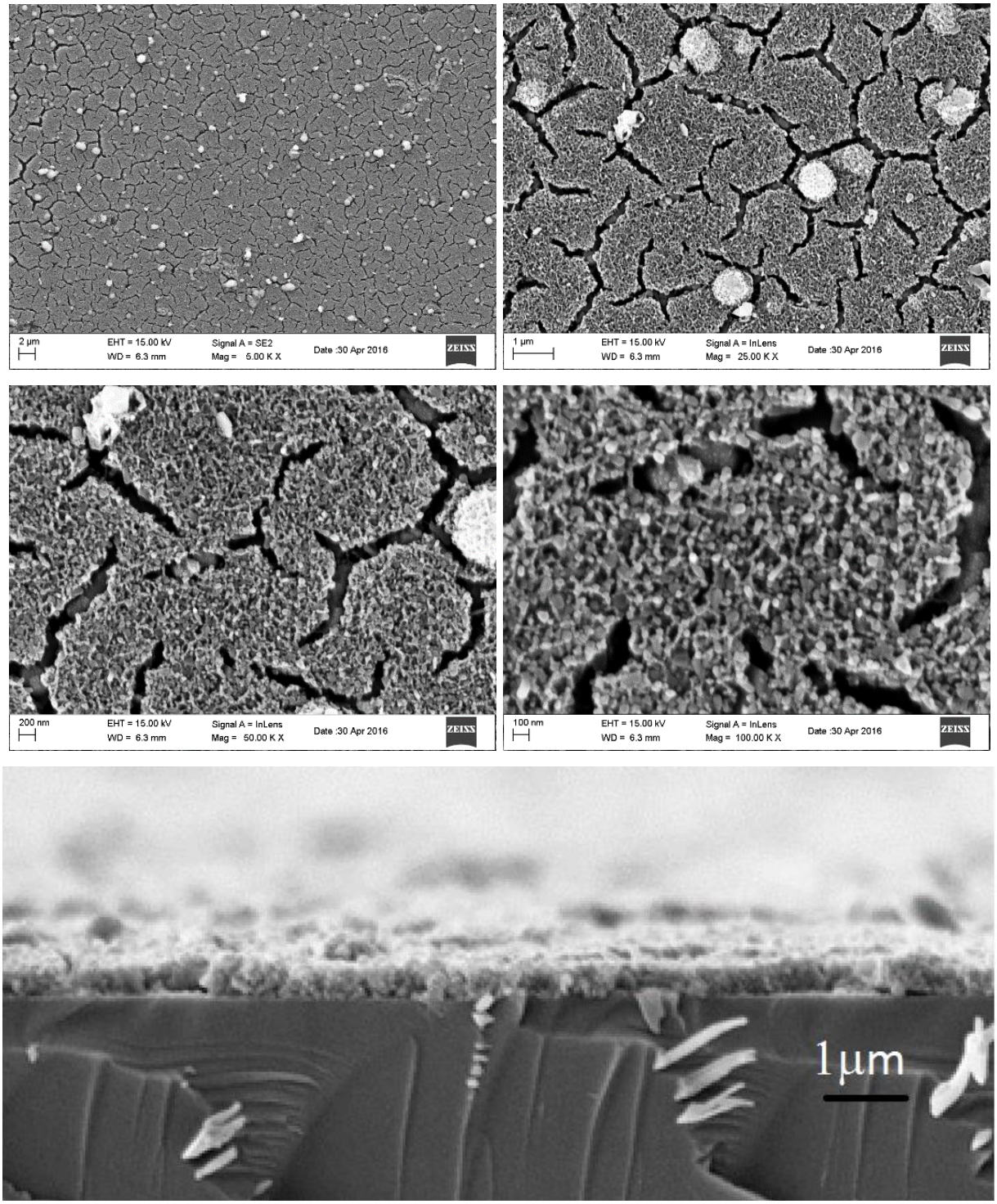

Figure 3.3: Typical surface and cross-sectional FESEM images of the film sulfurized at 400 ºC.

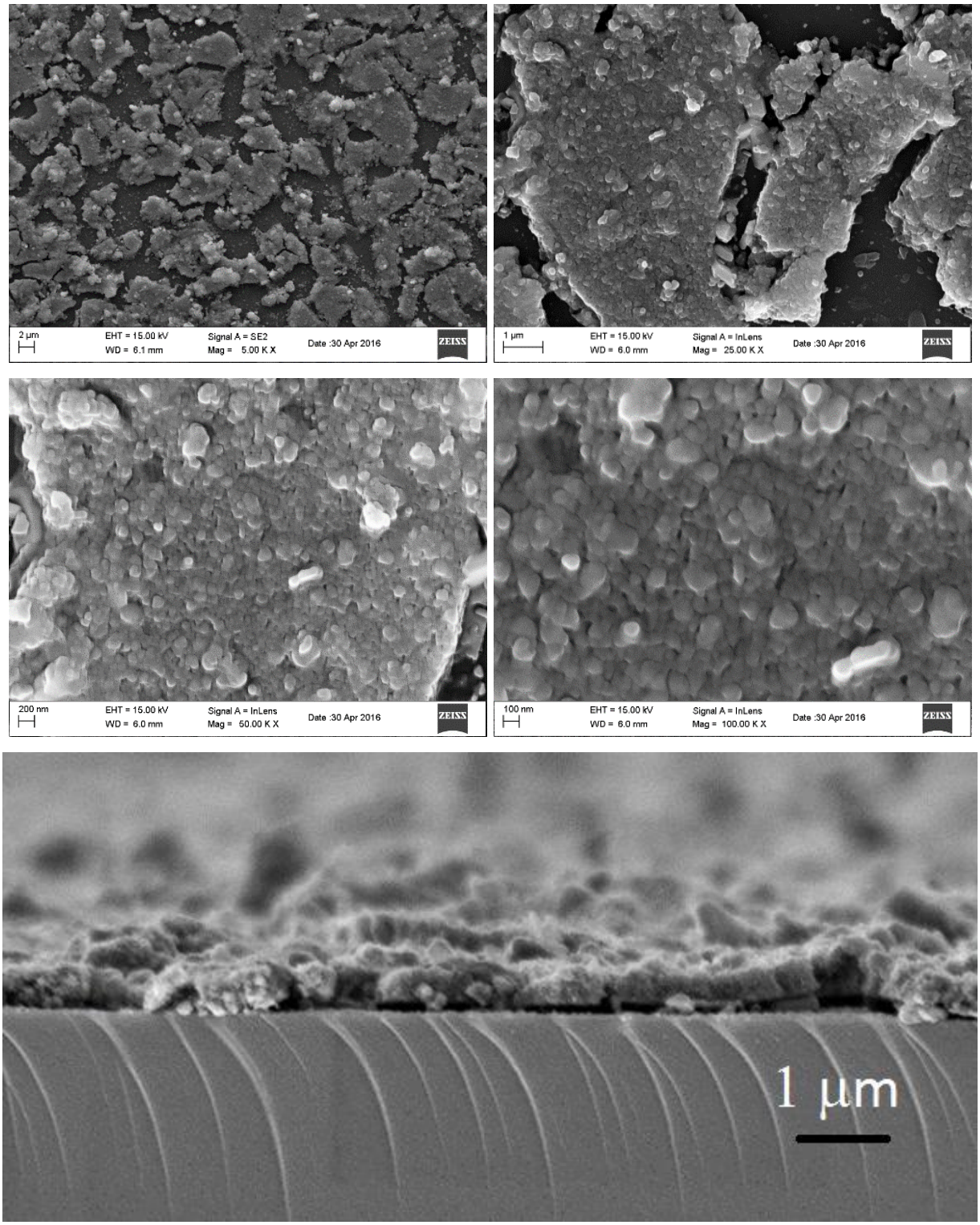

Figure 3.4: Typical surface and cross-sectional FESEM images of the film sulfurized at 450 ºC.

The sample sulfurized at 400 ºC still showed the mesh-like structure (as observed in the as-deposited sample), albeit improved compactness. At higher magnification, crystallization of the sample in the form of nearly-spherical particles were observed. The cross-sectional image showed that the thickness of the sample doubled to about 490 nm. However, there were many cracks in the films. Some of the cracks were isolated ones while many formed a continuous network in the films. As the sulfurization temperature was increased to 450 ºC, the mesh-like microstructure completely disappeared. The film was fully crystallized, as evident from higher magnification SEM micrographs. Locally, the film appeared to be well-crystallized. However, the film was completely discontinuous, and as the cross-sectional image shows, had been detached from the substrate at some places.

3.3 Optical studies

Optical properties of the as-deposited and sulfurized CZTS thin films were studied from the UV-visible transmittance curves. **Figures 3.5** shows typical transmittance curves of the films grown on the glass substrates.

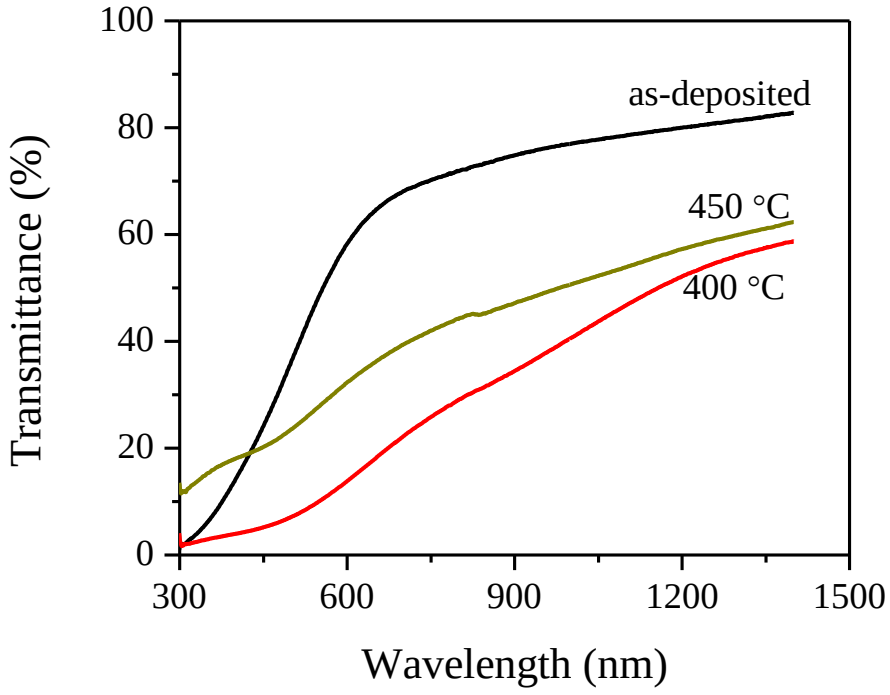

Figure 3.5 Optical transmittance curves of the as-deposited and sulfurized CZTS films.

The as-deposited film showed visible transmittance of around 80 % in the wavelength range of 600 – 1400 nm. The high transmittance could be due to the porous mesh-like microstructure as revealed from the SEM micrographs (Figure 3.2) that allowed much of the incident photons to pass through the film. Since the XRD measurement did not reveal formation of any crystalline phase, analysis of the spectrum to estimate the bandgap appears unwise. The film synthesized at 400 ºC, showed considerably lower transmittance, which is similar to the reports available in literature. However, the crystallinity of this film was poor as evidenced from low intensity Bragg peaks in the XRD pattern as well as from SEM micrographs. The film sulfurized at 450 ºC also showed a similar trend. Surprisingly, the sulfurized films showed significant transmittance in the small wavelength region, where it was expected to be nearly zero since the band gap of the CZTS is about 1.5 eV. However, no conclusion could be drawn with the limited data of XRD, SEM and the UV-visible transmittance.

CHAPTER 4
SUMMARY AND FUTURE SCOPE

The aim of this thesis was to fabricate and characterize Cu_2ZnSnS_4 (CZTS) thin films. As there are many methods to prepare the films, we used a cost-competitive method to prepare the films. Chemical bath deposition (CBD) technique is used for this purpose as it is easy to carry out, setup is inexpensive and large area deposition is possible. We have used copper chloride, zinc chloride, tin chloride and thioacetamine (TAA) as ion sources and MEA as stabilizing agent. Ethanol was used as the solvent. All films were deposited on soda lime glass (SLG) substrates for required temperature for definite time period. It was intended to prepare the films at relatively low temperature from the industrial point of view to reduce the cost. Different films are prepared using different annealing temperatures to obtain crystalline CZTS absorber layer. For characterization purpose various techniques such as XRD, FE-SEM and UV-visible spectroscopy are used.

From the XRD analysis, it is seen that on increasing annealing temperature, the polycrystallinity was improved. The results obtained at 450 ^{0}C are in good agreement with the standard results. The FE-SEM images showed that the as-deposited films had a mesh-like surface microstructure. However, at 450 ^{0}C, the mesh-like structure disappeared with the appearance of well-defined crystallites. From optical analysis, transmittance of the films was observed to be 80 % for as-deposited film in the wavelength range of 600-1400 nm.

The present work demonstrates that although coating from a single dip followed by sulfurization at 450 °C yields polycrystalline CZTS films, the films were discontinuous and had sub-micrometer particle size. Hence, further processing in the form of multiple coating is required for developing microstructure suitable for photovoltaic applications. The future scope of this work should include the optimization of process parameter including number of dip, duration of each dip, and post-deposition heat treatment.

References

[1]. Peter Wurfel. Physics of Solar Cells: From Principles to New Concepts. Weinheim: Wiley, 2005.

[2]. M. I. Khan, A. Kumar, A. Sharma and P. V. Singh. 2013, JECET, Vol. 2, p. 46.

[3]. G. D. Rai, Non-Conventional energy sources. New Delhi: Khanna, 2002.

[4]. R. F. Service. 2005, Science, Vol. 309, p. 548.

[5]. http://www.sc.doe.gov/bes/reports/files/SEU_rpt.pdf, Report of the Basic Energy Sciences Workshop on Solar Energy Utilization, US-DOE, April 18–21. 2005.

[6]. R. Eisenberg and D. G. Nocera. 2006, Inorg. Chem, Vol. 45, p. 6799.

[7]. A. R. Jha.Solar Cell Technology and Applications. Boca Raton: Auerbach, 2010.

[8]. M. A. Green. 2007, J Mater Sci: Mater Electron, Vol. 18, p. 15.

[9]. Lewis Fraas and Larry Partain, Solar cells and their applications. New Jersey: Wiley, 2010.

[10]. J. B. Li, V. Chawla and B. M. Clemens. 2012, Adv Mater, Vol. 24, p. 720.

[11]. B. R. Pamplin. 1960, Nature, Vol. 188, p. 136.

[12]. P. Jackson, D. Hariskos, R. Wuerz, W. Wischmann, M. Powalla, Physica Status Solidi (Rapid Research Letters) 8, 219 (2014).

[13]. http://investor.firstsolar.com/releasedetail.cfm?ReleaseID=828273

[14]. http://www.solar-frontier.com/eng/news/2012/C002980.html

[15]. http://investor.firstsolar.com/releasedetail.cfm?ReleaseID=833971

[16]. H. Katagiri, K. Jimbo, W. S. Maw, K. Oishi, M. Yamazaki, H. Araki, and A. Takeuchi, Thin Solid Films, 517, 2455 (2009).

[17]. D. B. Mitzi, O. Gunawan, T. K. Todorov, K. Wang, and S. Guha, Sol. Energy Mat. Sol. Cells, 95, 1421 (2011).

[18]. H. Katagiri, K. Jimbo, S. Yamada, T. Kamimura, W. S. Maw, T. Fukano, T. Ito, and T. Motohiro, Appl. Phys. Express, 1, 041201/1 (2008).

[19]. W. Wang, M. T. Winkler, O. Gunawan, T. Gokmen, T.K. Todorov, Y. Zhu, and D. B. Mitzi, Adv. Energy Mater., 4, 1301465 (2014).

[20]. L. A. Wahab, M. B. El-Den, A. A. Farrag, S. A. Fayek and K. H. Marzouk. 2009, J. Phys. Chem. Solids, Vol. 70, p. 604

[21]. J. Zhang, L. Shao, Y. Fu and E. Xie. 2006, Rare metals, Vol. 25, p. 315.

[22]. S. R. Hall, J. T. Szymanski and J. M. Stewart. The Canadian Mineralogist, 16(2), 131–137, 1978.

[23]. S. Schorr. 2007, Thin Solid Films, Vol. 515, p. 5985.

[24]. T. Maeda, S. Nakamura and T. Wada. 2009, In: Mater. Res. Soc. Symp. Proc., p. 1165.

[25]. S. R. Hall, J. T. Szymanski and J. M. Stewart. 1978, In: Canadian Mineralogist , Vol. 16, p. 131.

[26]. D. R. Lide.Handbook of Chemistry and Physics. 79th. s.l. : CRC press, 1998-1999.

[27]. T. Washio, H. Nozaki, T. Fukano, T. Motohiro, K. Jimbo and H. katagiri. 2011, J. Appl. Phys., Vol. 110, p. 074511.

[28]. S. Chen, J. Yang, X. G. Gong, A. Walsh and S. Wei. 2010, Phys. Rev. B, Vol. 81, p. 245204 (1).

[29]. J. Zhang and L. Shao. 2009, Sci. China Ser. E:Tech. Sci., Vol. 52, p. 269

[30]. Y. B. Kishore Kumar, P. uday Bhaskar, G. Suresh babu and V. Sundara raja. 2010, Phys. Status Solidi A , Vol. 207, p. 149.

[31]. N. Nakayama and K. Ito. 1996, Appl. Surf. Sci., Vol. 92, p. 171.

[32]. T. Tanaka, T. Nagatomo, D. kawasaki, M. Nishio, Q. Guo, A. Wakahara, A. Yoshida and H. Ogawa. 2005, J. Phys. Chem. Solids, Vol. 66, p. 1978.

[33]. K. Moriya, K. Tanaka and H. Uchiki. 2008, Jpn. J. Appl. Phys., Vol. 47, p. 602.

[34]. H. Katagiri, N. Sasaguchi, S. Hando, S. Hoshino, J. Ohashi and T. Yokota. 1997, Sol. Energy Mater. Sol. Cells, Vol. 49, p. 407.

[35]. T. K. Chaudhari and D. Tiwari. 2012, Sol. Energy Mater. Sol. Cells, Vol. 101, p. 46.

[36]. P. A. Fernandes, P. M. P. Salome, A. F. da Cunha and B. Schubert. 2010, Thin Solid Films, Vol. 519, p. 7382.

[37]. V. G. Rajeshmon, C. Sudha Kartha, K. P. Vijayakumar, C. Sanjeeviraja, T. Abe and Y. Kashiwaba. 2011, Sol. Energy, Vol. 85, p. 249.

[38]. K. Ito and T. Nakazawa. 1988, Jpn. J. Appl. Phys., Vol. 27, p. 2094.

[39]. F. Liu, Y. Li, K. Zhang, B. Wang, C. Yan, Y. Lai, Z. Zhang, J. Li and Y. Liu. 2010, Sol. Energy Mater. Sol. Cells, Vol. 94, p. 2431.

[40]. C. P. Chan, H. Lam and C. Surya. 2010, Sol. Energy Mater. Sol. Cells, Vol. 94, p. 207.

[41]. W. Xinkun, L. Wei, C. Shuying, L. Yunfeng and J. Hongjie. 2012, J. Semicond., Vol. 33, p. 022002.

[42]. S. Chen, X. G. Gong, A. Walsh and S. Wei. 2009, Appl. Phys. Lett., Vol. 94, p. 041903.

[43]. J. Seol, S. Lee, J. Lee, H. Nam and K. Kim. 2003, Sol. Energy mater. Sol. Cells, Vol. 75, p. 155.

[44]. K. Moriya, J. Watabe, K. Tanaka and H. Uchiki. 2006, Phys. status solidi (c), Vol. 3, p. 2848.

[45]. K. Sekiguchi, K. Tanaka, K. Moriya and H. Uchiki. 2006, Phys. status solidi (c), Vol. 3, p. 2618.

[46]. T. Prabhakar and J. Nagaraju. s.l. : Proceedings of the IEEE 35th Photovoltaic Specialist Conference,Hawaii, USA, 2010. p. 1964.

[47]. K. Tanaka, N. Moritake, M. Oonuki and H. Uchiki. 2008, Jpn. J. Appl. Phys., Vol. 47, p. 598.

[48]. P. A. Fernandes, P. M. P. Salome and A. F. da Cunha. 2011, J. Alloys Compd., Vol. 509, p. 7600.

[49]. Y. Cui, S. Zuo, J. Jiang, S. Yuan and J. Chu. 2011, Sol. Energy Mater. Sol. Cells, Vol. 95, p. 2136.

[50]. J. P. Leitao, N. M. Santos, P. A. Fernandes, P. M. P. Salome, A. F. da Cunha, J. C. Gonzalez, G. M. Ribeiro and F. M. Matinaga. 2011, Phys. Rev. B, Vol. 84, p. 024120.

[51]. J. P. Leitao, N. M. Santos, P. A. Fernandes, P. M. P. Salome, A. F. da Cunha, J. C. Gonzalez and Fs. M. Matinaga. 2011, Thin Solid Films, Vol. 519, p. 7390.

[52]. K. Ito, T. Nakazawa, Jpn. J. Appl. Phys. 27, 2094 (1988).

[53]. H. Katagiri, N. Sasaguchi, S. Hando, S. Hoshino, J. Ohashi, and T. Yokota, Sol. Energy Mater. Sol.Cells, 49, 407 (1997).

[54]. T. M. Friedlmeier, N. Wieser, T. Walter, H. Dittrich, and H. W. Schock, p. 1242, Bedford, UK, 1997.

[55]. H. Katagiri, et al., Tech. Dig. Photovoltaic Science and Engineering Conf.-11, Sapporo, (1999) p.647.

[56]. H. Katagiri, et al., Proc. World Conf. on Photovoltaic Energy Conversion-3, Osaka, (2003) p. 2874.

[57]. K. Todorov, K. B. Reuter, and D. B. Mitzi, Advanced Materials, vol. 22, no. 20, pp. E156–E159, 2010. View at Publisher · View at Google Scholar · View at Scopus

[58]. Q. Guo, H. W. Hillhouse and R. Agrawal, J. Am. Chem. Soc., 131, 11672 (2009).

[59]. Q. Guo, G. M. Ford, W.-C. Yang, B. C. Walker, E. A. Stach, H. W. Hillhouse, and R. Agrawal, J. Am. Chem. Soc., 132, 17384 (2010).

[60]. M. G. Panthani, V. Akhavan, B. Goodfellos, J. P. Schmidtke, L. Dunn, A. Dodabalapur, P. F. Barbara and B. A. Korgel, J. Am. Chem. Soc., 130, 16770 (2008).

[61]. A. Fischereder, T. Rath, W. Haas, H. Amenitsch, J. Albering, D. Meischler, S. Larissegger, M. Edler, R. Saf, H. Hofer and G. Trimmel, Chem. Mater., 22, 3399 (2010).

[62]. W. Ki and H. W. Hillhouse, Adv. Energy Mater., 1, 732 (2011).

[63]. M. Krunks, V. Mikli, O. Bijakina, H. Rebane, A. Mere,T. Varema and E. Mellikov, Thin Solid Films, **361**, 61 (2000).

[64]. Y. Sun, Y. Zhang, H. Wang, M. Xie, K. Zong, H. Zheng, Y. Shu, J. Liu, H. Yan, M. Zhu and W. Lau, J. Mater. Chem. A, 1, 6880 (2013).

[65]. C. M. Sutter-Fella, J. A. Stückelberger, H. Hagendorfer, F. La Mattina, L. Kranz, S. Nishiwaki, A. R. Uhl, Y. E. Romanyuk, and A. N. Tiwari, Chem. Mater. 26, 1420 (2014).

[66]. Z. Tong, C. Yan, Z. Su, F. Zeng, J. Yang, Y. Li, L. Jiang, Y. Lai and F. Liu, Appl. Phys. Lett., 105, 223903 (2014).

[67]. S. N. Park, S. J. Sung, D. H. Son, D. H. Kim, M. Gansukh, H. Cheong and J. K. Kang, RSC Adv., 4, 9118 (2014).

[68]. V. T. Nguyen, D. Nam, M. Gansukh, S. Park, S. J. Sung, D. H. Kim, J. K. Kang, C. D. Sai, T. H. Tran, and H. Cheong, Solar Energy Materials and Solar Cells 136, 113 (2015).

[69]. Yang, Y., Kang, X., Huang, L., Wei, S., & Pan, D. Journal of Power Sources, 313, 15(2016).

[70]. Prabeesh, P., Selvam, I. P., & Potty, S. N. (2016). Thin Solid Films, 606, 94(2016).

[71]. http://particle.dk/methods-analytical-laboratory/xrd-analysis/

[72]. http://www.vcbio.science.ru.nl/public/pdf/fesem_info_eng.pdf

[73]. A. Mehta, “UV-Vis Spectroscopy- Limitations and Deviations of Beer- Lambert Law”, Analytical Chemistry (2012).

[74]. P. Misra and M. A. Dubinskii, “Ultraviolet Spectroscopy and Uv- Lasers”, New York, Marcel Dekker (2002).

[75]. B. W. Kempshall, L. A. Giannuzzi, B. I. Prenitzer, F. A. Stevie and S. X. Da, J. Vacuum Sci. Technol. B 20, 286 (2002).